SuperNova, a monomeric photosensitizing fluorescent protein for chromophore-assisted light inactivation

Kiwamu Takemoto, Tomoki Matsuda, Naoki Sakai, Donald Fu, Masanori Noda, Susumu Uchiyama, Ippei Kotera, Yoshiyuki Arai, Masataka Horiuchi, Mareo Fukui, Tokiyoshi Ayabe, Fuyuhiko Inagaki, Hiroshi Suzuki and Takeharu Nagai

Supplementary Information

Supplementary Results

Analytical ultracentrifugation sedimentation equilibrium analysis

Overall structure of SuperNova

Interface of the crystallographic dimer of SuperNova

Structure around the chromophore

Supplementary Figure 1

Basic properties of SuperNova

Supplementary Figure 2

Sedimentation equilibrium analytical ultracentrifugation

Supplementary Figure 3

Crystal structure of SuperNova

Supplementary Figure 4

Confocal images of SuperNova fusion proteins expressed in HeLa cells

Supplementary Figure 5

Effects of KillerRed expression on endogenous function of mechanosensory neurons in *C. elegans*

Supplementary Figure 6

Measurements of phototoxic activity

Supplementary Figure 7

Induction of apoptotic cell death in HeLa cells expressing SuperNova in their mitochondria

Supplementary Table

Data collection and refinement statistics

Supplementary Movie 1

Motility of actin filaments before CALI with cofilin-SuperNova in *COS7 cell*

Supplementary Movie 2

Motility of actin filaments after CALI with cofilin-SuperNova in *COS7 cell*

SUPPLEMENTARY RESULTS

Analytical ultracentrifugation sedimentation equilibrium analysis.

Sedimentation equilibrium experiments were performed on a Beckman Optima XL-I analytical ultracentrifuge at 20°C using interference optics. Samples of each protein at several concentrations (KillerRed: 5 μM, 25 μM, 50 μM; SuperNova and mCherry: 10 μM, 50 μM, 100 μM) were loaded into 6-channel epon centerpieces. Samples were centrifuged at 20,000 rpm. The data were analyzed by nonlinear least-squares analysis using the software package (Microcal Origin) supplied by Beckman. The goodness of fit was evaluated on the basis of the magnitude and randomness of the residuals, expressed as the difference between the experimental data and the theoretical curve and also by checking each of the fit parameters for physical reasonability. The molecular mass calculated using SEDNTERP v 1.09 was employed for the estimation of dissociation constants.

Concentration dependences of apparent molecular weights clearly indicated that KillerRed, SuperNova and mCherry does in fact undergo a dimer-to-monomer transition (**Supplemental Figure 1**). The dissociation constants of 3.0 μM for KillerRed, 980 μM for SuperNova and 1.62 mM for mCherry were estimated from the sedimentation equilibrium concentration gradients for 50 μM (KillerRed) and 100 μM (SuperNova and mCherry) solutions. Although these values for SuperNova and mCherry may not be accurate because the values were derived without considering the non-ideality effect (which couldn't be negligible for AUC-SE distribution of 100 μM

solution), the results AUC-SE analysis indicate that KillerRed has higher dimerization affinity than SuperNova and mCherry.

Overall structure of SuperNova.

The structure of SuperNova was determined at 2.3-Å resolution by the molecular replacement method using the coordinates of the protomer of KillerRed, which was solved by our group (PDB ID: 3A8S), as a search model. The details of data collection and refinement are summarized in **Supplementary Table**. SuperNova was composed of an 11-stranded β-barrel with an internal α-helix passing through the inside of the barrel, which is characteristic of the fluorescent protein family (**Supplementary Figure 2**). The chromophore is formed by the autocatalytic cyclization and oxidation of 3 residues (Gln65-Tyr66-Gly67) located at the center of the internal α-helix. The crystal structure of SuperNova was determined to be a dimer. The final model contains 8 SuperNova monomers (4 dimers) in the crystal lattice. The root-mean-square deviation (RMSD) values between independent monomers ranged from 0.166 to 0.357. The N-terminal residues, C-terminal tail, and residues composing the loop between β10 and β11 were disordered. Residues 5–206 and 214–228 were present in all the SuperNova monomers.

The dimer interface consists of hydrophilic (Arg97, Glu99, Ser145, Glu146, His148, Arg158, Thr160, Thr162, Gly164, Lys172, His176, Thr198, Thr201, Lys202, Arg217, Glu218, His223, and Arg227) and hydrophobic moieties (Leu143, Pro144, Phe150, Pro151, Ala161, Met174, Pro194, Phe196, Ile200, Val219, Tyr221, Val225,

Pro226, and Ile228). The C-terminal extension (His223-Ile228) was involved in the interchain interaction in a hydrophobic manner.

Interface of the crystallographic dimer of SuperNova.

To decrease the dimeric state of KillerRed, Leu160 and Phe162, which faced the dimeric surface and contacted each chain, were substituted with threonine (Thr160 and Thr1624, respectively, in SuperNova). Because of these mutations, KillerRed-L160T/F162T was monomeric in solution (**Figure 1 and 2**). In the crystal structure of SuperNova, a change in the dimer orientation of KillerRed was observed (**Supplementary Figure 2b**). Thr160 and Thr162 have no hydrogen bond connection with any atoms in other chains. The distance between the Cα atoms of L160 of KillerRed is 11.6 Å; however, the distance between the Cα atoms of Thr160 in SuperNova is 14.0 Å (**Supplementary Figure 2c, d**). This means that the dimer packing of SuperNova is changed in its crystal structure. In the results upon mutation on these residues, which comprised the dimer interface of KillerRed, the averaged dimer interface area of 8 SuperNova chains in an asymmetric unit is 1131.3 $Å^2$, which is less than that of KillerRed (1654.9 $Å^2$ for chain A and 1671.6 $Å^2$ for chain B)[9]. This reduction of the interface area is considered to be due to the mutation in the central keel of the dimer interface composed of the hydrophobic stacks of Leu160 and Phe162 of both chains in KillerRed (**Supplementary Figure 2d**). This suggests that the dimer of SuperNova in the crystal is formed by high concentrations of SuperNova in the crystallization process.

In KillerRed, the dimer interface is stabilized via 2 salt bridges between the side chains of Glu99 and Arg158 (**Supplementary Figure 2d**). However, in SuperNova, the salt bridges between the side chains of Glu99 and Arg158 were not detected in the electron density map (**Supplementary Figure 2c**).

The crystal structure of SuperNova presented in this study existed as a dimer; however, compared with the dimer orientation of KillerRed, the propensity to form a dimer is reduced in SuperNova. In the *P*1 crystal of SuperNova, there are 4 noncrystallographic dimers in a unit cell. In a solution state, SuperNova exists as a monomer with a dissociation constant exceeding 100 μM, which was confirmed by analytical ultracentrifugation. The previous structural study of Pletnev et al.[9] indicated that the extended C-terminal tail region contributes to the stabilization of the dimer interface. In SuperNova, C-terminal extension was also observed, and no mutation was detected in this region during the engineering to produce SuperNova. This C-terminal extension may induce the dimer formation observed in the crystal structure of SuperNova.

Structure around the chromophore.

In dimeric KillerRed, the phenolate oxygen of the chromophore is stabilized by a hydrogen bond between the side chain amine of Asn145. This asparagine was mutated from threonine in the development of KillerRed, which was derived from the nonfluorescent protein anm2CP. The T145N mutation is required for the fluorescent property and phototoxic activity of KillerRed[10]. Because the amine of the asparagine

side chain tightly interacts with the phenolate oxygen of the chromophore, the conformation of the chromophore is stabilized in the fluorescent *cis* conformation of KillerRed. In SuperNova, this residue is mutated to serine (Ser145), which lacks the amine required for the hydrogen bond. Therefore, the phenolate oxygen is considered unstable. However, the B-factor of this phenolate oxygen is low. In SuperNova, the phenolate oxygen of the chromophore is stabilized by the hydrogen bond network via a conserved water molecule. This hydrogen bond network among the main chain oxygen of Leu143, main chain oxygen of Ile199, side chain hydroxy group of Thr201, and the chromophore phenolate oxygen via a water molecule stabilizes the fluorescent *cis* conformation of the chromophore. A mutation at 201 from isoleucine to threonine was required to create KillerRed. The side chain hydroxyl moiety is probably the H-bond acceptor.

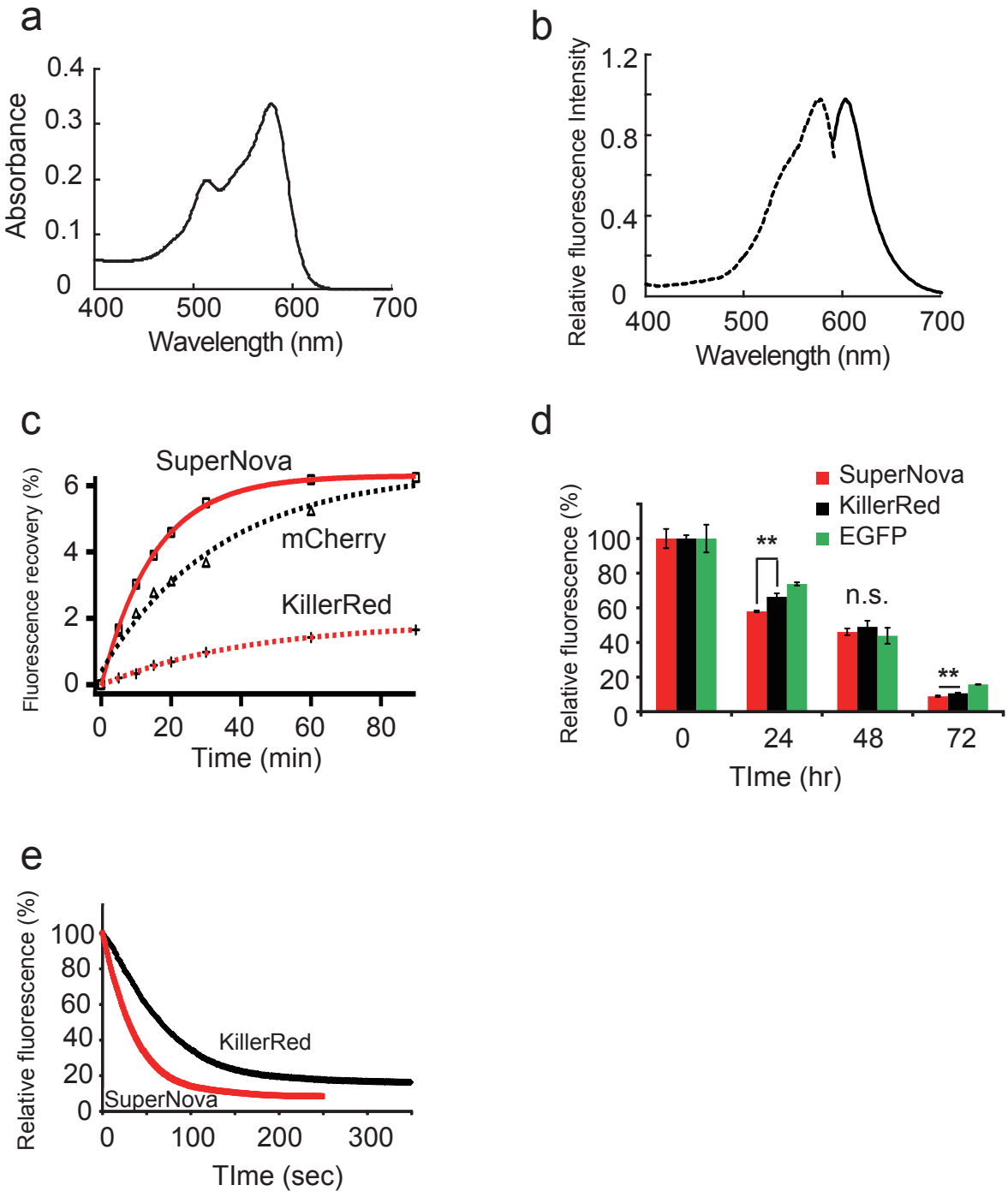

Supplementary Figure 1. Basic properties of SuperNova. (**a**) Absorption spectrum of SuperNova. (**b**) Excitation (dotted line) and fluorescence (solid line) spectra of SuperNova. (**c**) Refolding and reoxidation of SuperNova, mCherry and KillerRed in vitro. (**d**) Stability of SuperNova in living HeLa cells. n=3, **p<0.05 (t-test) (**e**) Photobleaching assay of SuperNova and KillerRed. Fluorescence decrease (%) in responce to strong laser exposure (543nm) were detected and typical results were averaged (n=4 cells).

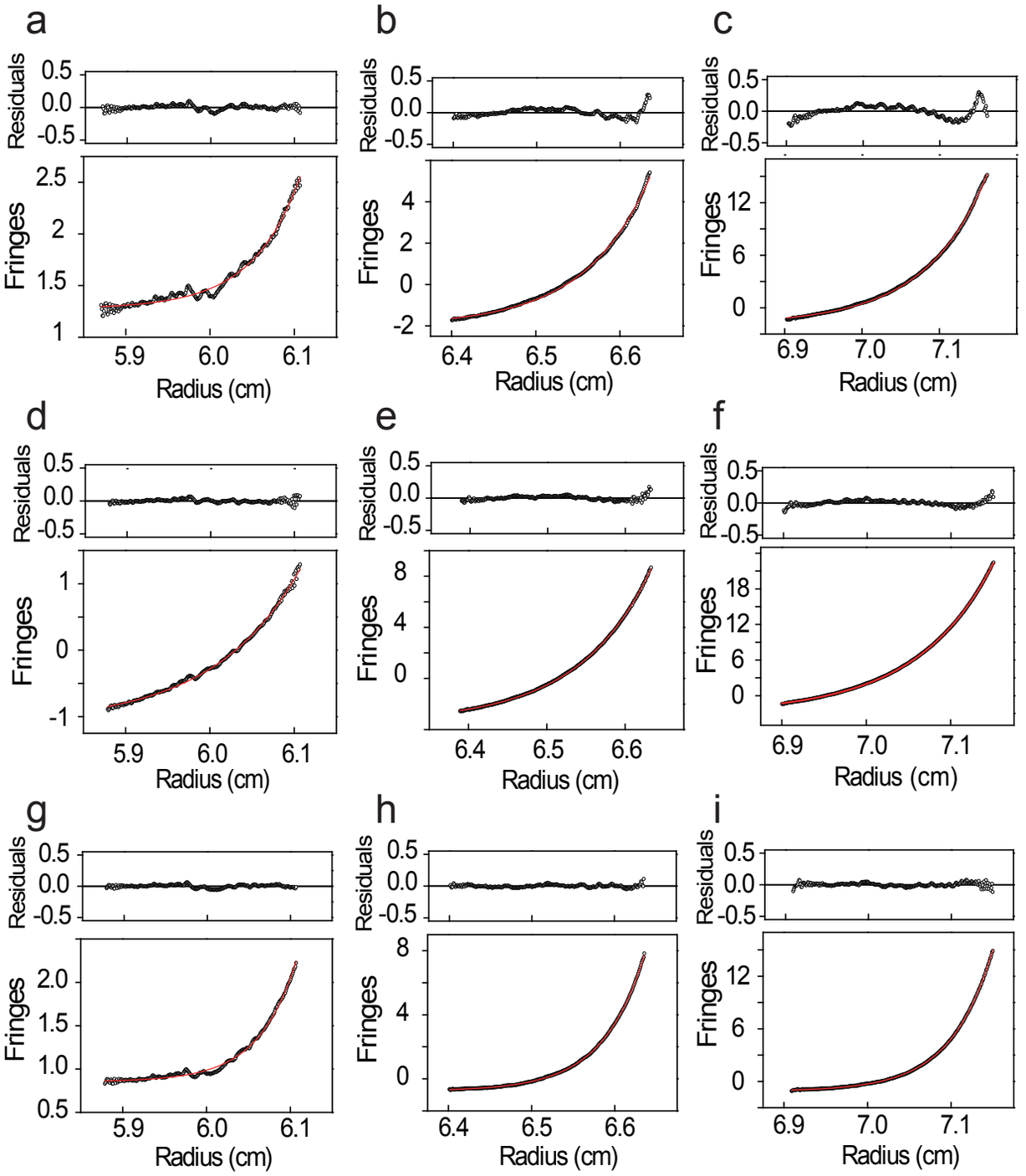

Supplementary Figure 2. Sedimentation equilibrium analytical ultracentrifugation. SuperNova (**a-c**), mCherry (**d-f**) and KillerRed (**g-i**). Samples at several concentrations (SuperNova and mCherry: 10 μM (**a, d**), 50 μM (**b, e**), 100 μM (**c, f**); KR: 5 μM (**g**), 25 μM (**h**), 50 μM (**i**)) were loaded and centrifuged at 20,000 rpm at 20°C. The data were analyzed by nonlinear least-squares analysis (red line). The residual differences between the predicted distribution and data are shown in upper panels.

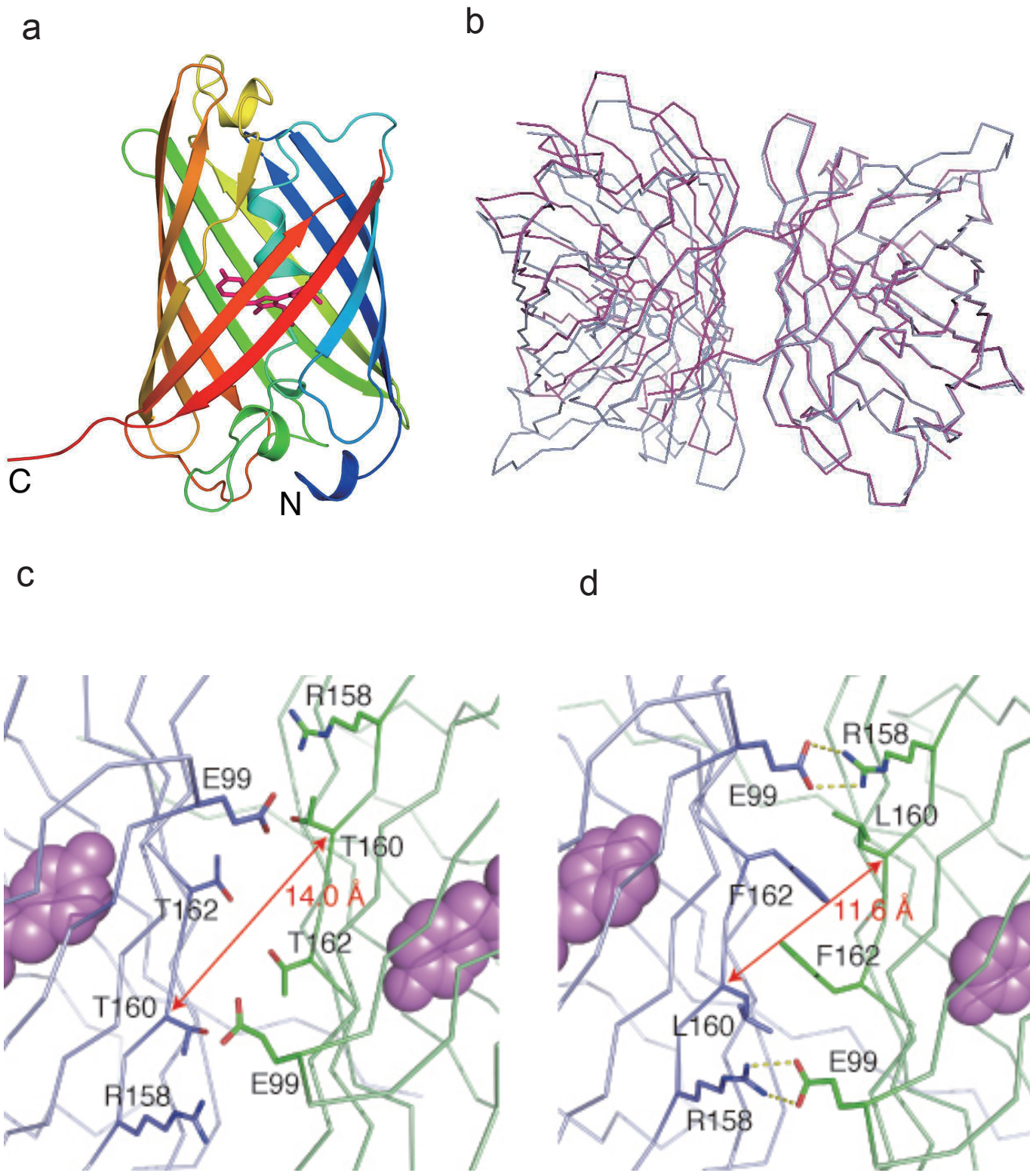

Supplementary Figure 3. Crystal structure of SuperNova. (**a**) The SuperNova monomer is represented by a rainbow ribbon diagram, and the chromophore is represented by the magenta stick model. (**b**) Structural alignment of the crystallographic dimer of SuperNova (magenta) and KillerRed (3GB3, in purple). One chain is aligned with the minimum RMSD of the Cα chain. (**c**) Dimer interface of SuperNova. The corresponding residues, which are involved in the dimer interaction in KillerRed, are shown in the stick model. Chain A is shown in purple, and B is shown in green, and the chromophore is shown as the space-filling model. (**d**) Dimer interface of KillerRed. Hydrogen bonds are shown as yellow dashes. This figure was produced from the PDB coordinate of 3GB3. The residues, which interact with another chain, are shown in the stick model. The color and model schemes are the same as in (**c**).

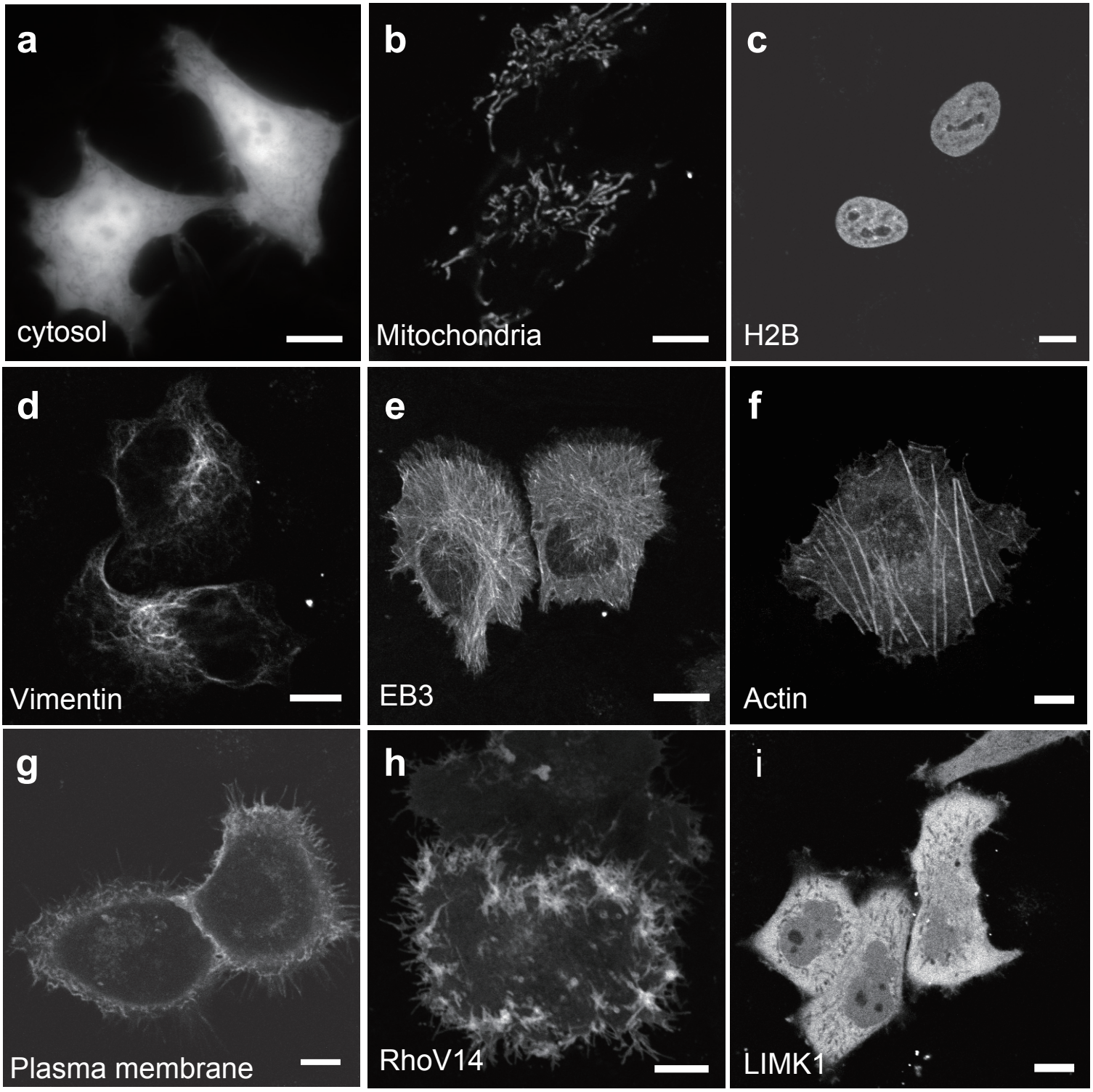

Supplementary Figure 4. Confocal images of SuperNova fusion proteins expressed in HeLa cells. (a) SuperNova was evenly distributed in the cytosol and nucleus without any visible aggregates or nonspecific localization. The SuperNova fusion proteins for SuperNova-Mitochondria (b), SuperNova-H2B, a core histone protein localized in nuclei (c), Vimentin-SuperNova. Fuion to vimentin is highlighting intermediate filament (d), EB3-SuperNova. Fusion to EB3 is highlighting microtubules throughout cytoplasm and that there is a distinct absence within nuclei (e), Actin-SuperNova. Actin is a cytoskeletal protein so that fusion to actin highlights actin fibers in cytosol (f), Lyn-SuperNova. Lyn is a sigal sequence for plasma membrane localization so that fusion protein was stronlgly localized in plasmaembrane (g), SuperNova-RhoV14, a constitutive active Rho that is localized in plasma membrane (h), and LIMK1-SuperNova. LIMK1 is a cytosolic kinase for cofilin so that cytosol should be highlighted by its fusions (i) were expressed in HeLa cells. Scale bars, 10 μm.

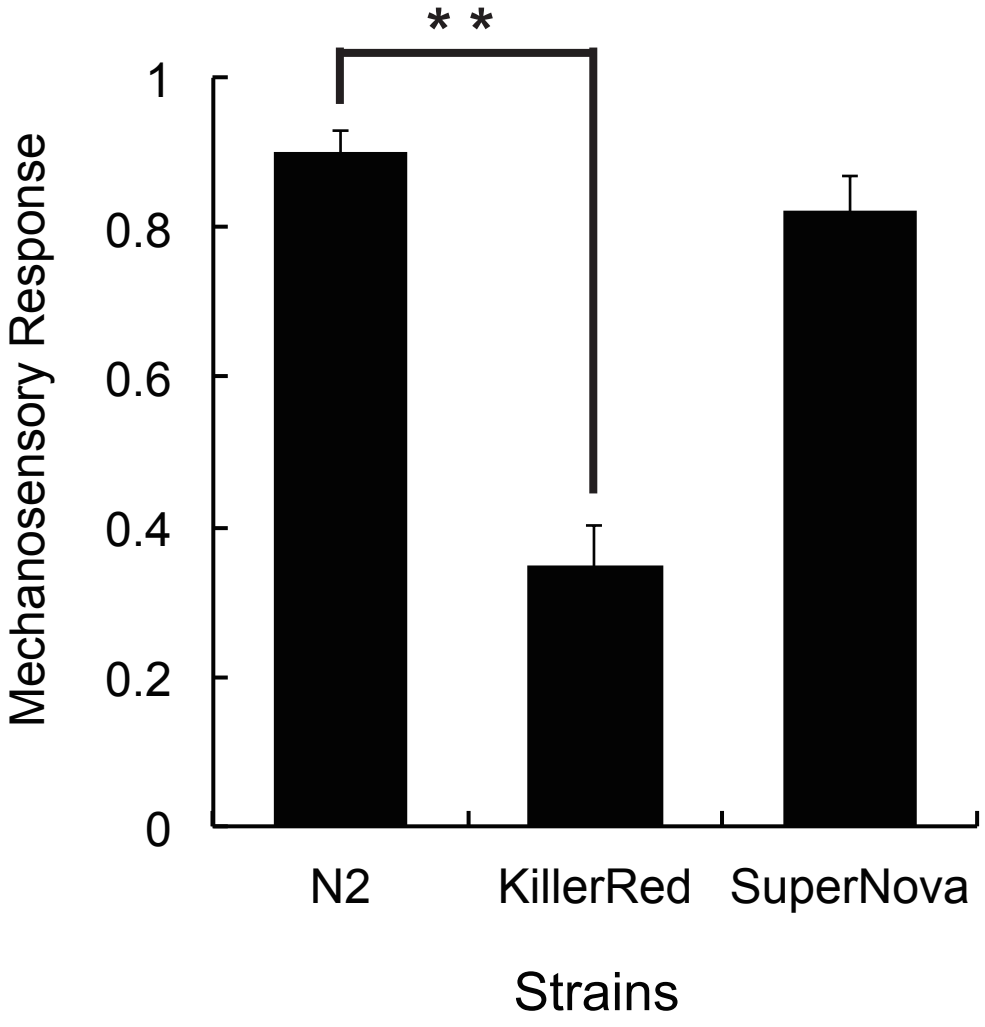

Supplementary Figure 5. Effects of KillerRed expression on endogenous function of mechanosensory neurons in *C. elegans*. KillerRed impaired neuronal function, whereas the SuperNova did not.

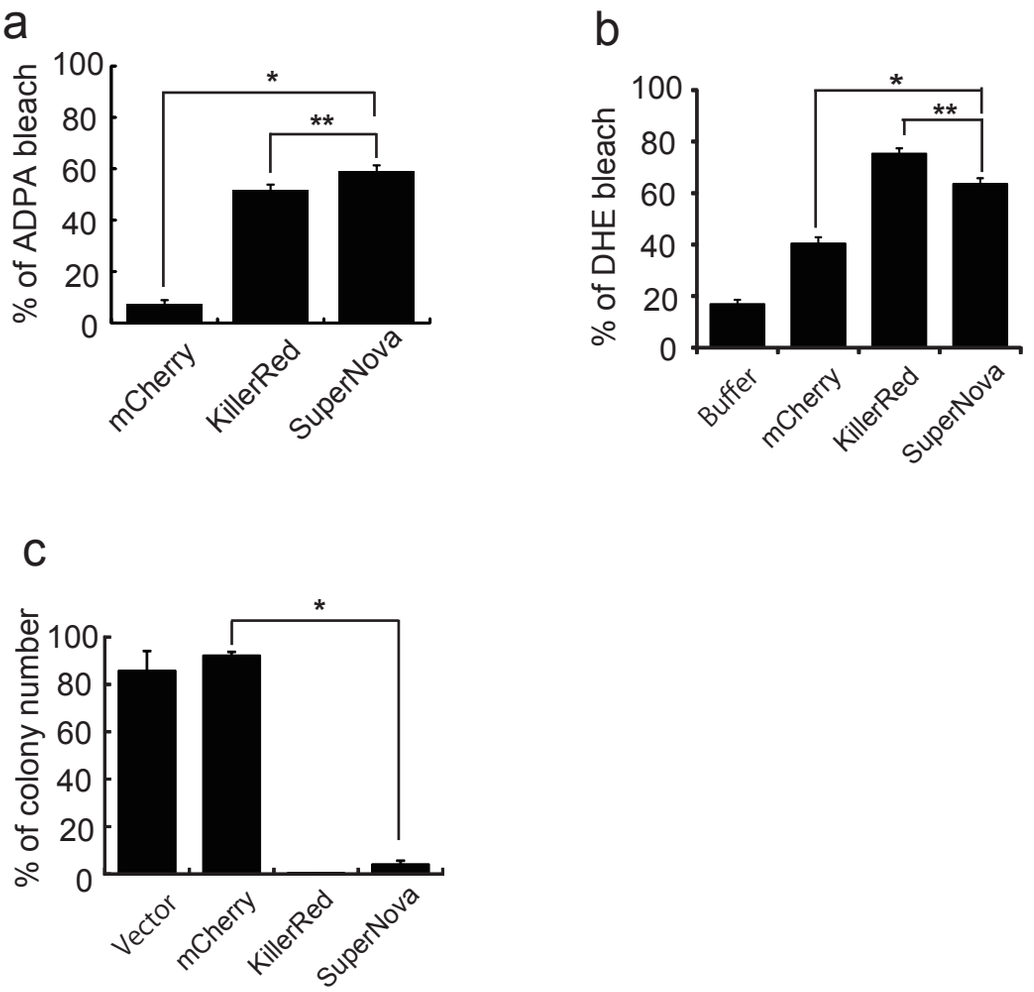

Supplementary Figure 6. Measurements of phototoxic activity. (**a**) Measurement of singlet oxygen generation in samples containing mCherry, KillerRed, or SuperNova proteins by detection of bleaching in ADPA fluorescence. Light irradiation was examined by 1.4 W/cm2, 5 min. n=4, *p<0.01, **p<0.05(t-test). (**b**) Measurement of superoxide generation in samples containing Buffer, mCherry, KillerRed or SuperNova by detection of bleaching in dihydroethidium fluorescence. Light irradiation was examined by 0.73W/cm2, 10min. n=4, *p<0.01, **p<0.05(t-test). (**c**) Phototoxicity of SuperNova by CALI in *E. coli*. With CALI (CALI+) and without CALI (CALI-) was compared and shown as "% colony number".

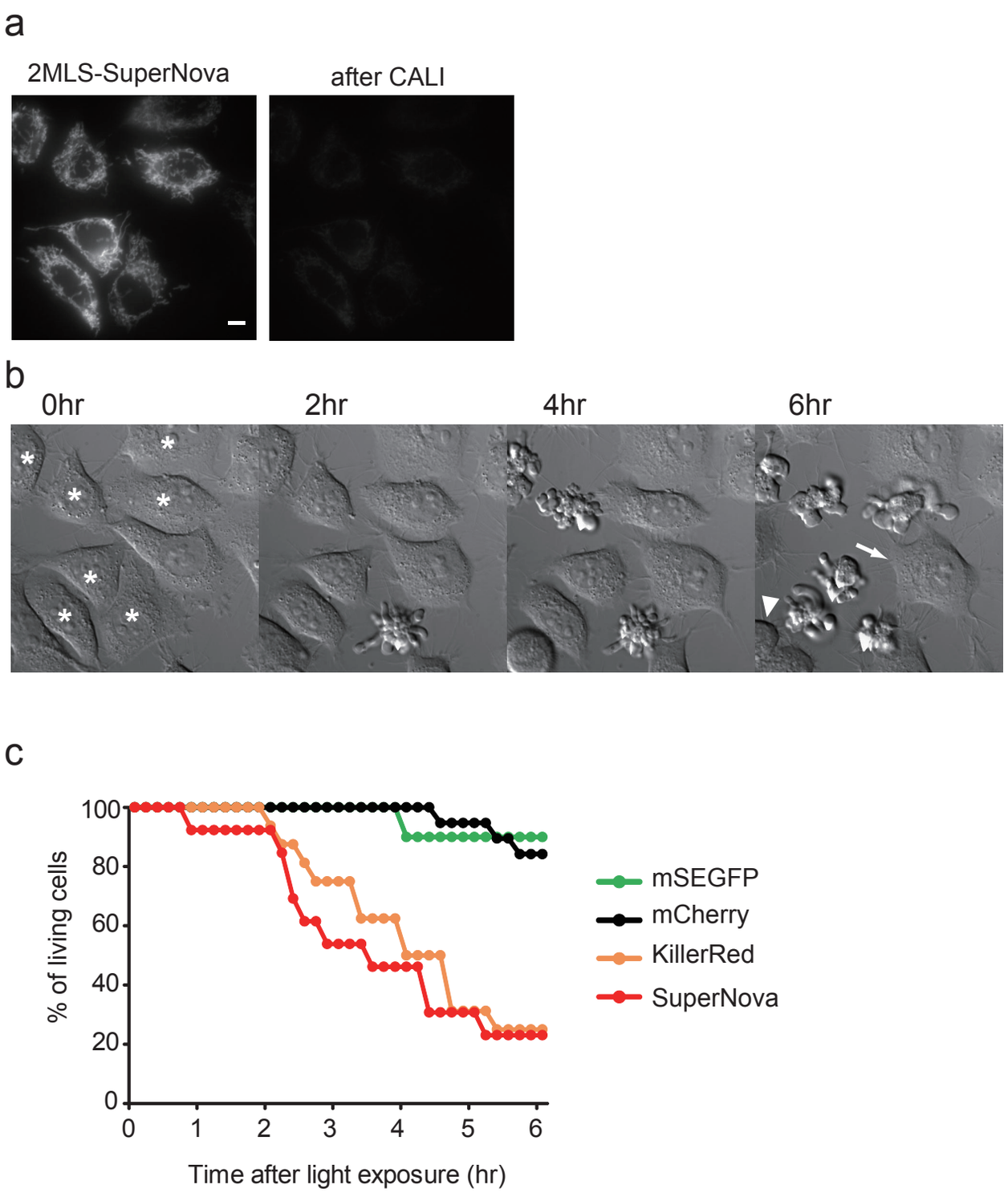

Supplementary Figure 7. Induction of apoptotic cell death in HeLa cells expressing SuperNova in their mitochondria. (**a**) Image of a fluorescent HeLa cell before (left panel) and after (right panel) intense green light exposure. (**b**) Time-lapse DIC images of HeLa cells after intense light exposure. Asterisks indicate SuperNova expressing cells. After 6 hrs, almost all of SuperNova expressing cells were dead (6/7cells). In contrust, SuperNova negative cells (arrow and arrowhead) were still living. Note that one SuperNova negative cell (arrowhead) devide to doughter cells between 4-6 hr. (**c**) Time course of cell viability after CALI. The number of surviving HeLa cells expressing mSEGFP (green), mCherry (black), KillerRed (Orange), and SuperNova (red) in mitochondria were counted after intense light irradiation (mercury lamp with 580AF20 filter, 8 W/cm2, 60sec). The phototoxic efficiency of SuperNova is superior to that of KillerRed (n=13,16 cells, respectively; $p<0.0001$ by Wilcoxon test). Scale bars, 10 μm.

Supplementary Tabale Data collection and refinement statistics

Data collection	
Space group	*P*1
Cell dimensions	
a, *b*, *c* (Å)	60.3, 89.3, 109.9
α, β, γ (°)	70.6, 89.9, 71.6
Resolution (Å)	50.0 – 2.30 (2.34 – 2.30) *
R_{sym}	0.070 (0.323)
$<I / \sigma(I)>$	23.5 (5.1)
Completeness (%)	97.9 (97.1)
Redundancy	3.1 (3.1)
Refinement	
Resolution (Å)	20.0 – 2.3
No. reflections	83631
R_{work} / R_{free}	0.181 / 0.235
No. atoms	14303
Protein	13795
Ligand/ion	0
Water	508
Average B value (Å^2)	28.096
R.m.s. deviations	
Bond lengths (Å)	0.019
Bond angles (°)	1.942

1 crystal was used for structure analysis